An *in situ* colorimetric measurement study of electrochromism in the di-*n*-heptyl viologen system

Roger J. Mortimer[†], John R. Reynolds

The George and Josephine Butler Polymer Research Laboratory, Department of Chemistry, Center for Macromolecular Sciences and Engineering, University of Florida, Gainesville, Florida 32611, USA

Abstract

An *in situ* colorimetric method, based on the CIE (Commission Internationale de l'Eclairage) system of colorimetry, has been applied to the study of the electrochromic *N*,*N*´-bis(*n*-heptyl)-4,4´-bipyridylium ('di-*n*-heptyl viologen') system in aqueous solution on transmissive ITO/glass substrates. On electrochemical reduction of the di-*n*-heptyl viologen di-cation, the purple di-*n*-heptyl viologen radical cation salt deposits as a film and the changes in hue and saturation have been tracked using CIE 1931 *xy* chromaticity coordinates. The CIELAB 1976 colour space coordinates of the purple di-*n*-heptyl viologen radical cation salt were $L^* = 76$, $a^* = 33$ and $b^* = -20$, with a complementary wavelength of 548 nm. A sharp decrease in luminance was found on formation of the di-*n*-heptyl viologen radical cation salt. Colour coordinates for the reverse (oxidation) direction plots show hysteresis, implying that specific choice of colour values depends on both the potential applied and from which direction the potential is changed.

Keywords: Electrochromic; electrochromism; CIE colour coordinates; colorimetry; *N*,*N*´-bis(*n*-heptyl)-4,4´-bipyridylium; di-*n*-heptyl viologen

[†] Corresponding author. Permanent address: Department of Chemistry, Loughborough University, Loughborough, Leicestershire LE11 3TU, UK. Tel.: +44 1509 222 583; fax: +44 1509 223 925.
E-mail address: R.J.Mortimer@lboro.ac.uk (R.J.Mortimer)

1. Introduction

Electrochromism is a change, evocation, or bleaching, of colour as effected either by an electron-transfer (redox) process or by a sufficient electric potential [1]. Visible electrochromism is only useful for display purposes if one of the colours is markedly different from the other, as for example when the absorption band of one redox state is in the visible region of the electromagnetic spectrum, while the other is in the UV. If the colours are sufficiently intense and different, then the material is said to be electrochromic and the species undergoing change is usefully termed an 'electrochrome' [1]. Many chemical species show electrochromic properties [1–3], including metal coordination complexes, both in solution and as polymer films, inorganic charge-transfer complexes, metal oxides (especially tungsten trioxide, WO_3), viologens (4,4´-bipyridylium salts) and conjugated conducting polymers such as polypyrroles and polythiophenes.

Colour [4, 5] is a subjective phenomenon, causing the description of colour difference or the comparison of two colours to be quite difficult. However, much effort has been given to the development of *colorimetric analysis*, which allows a quantitative description of colour and relative transmissivity as sensed by the human eye. Colorimetry provides a more precise way to define colour than spectrophotometry [6]. Rather than record absorption bands, in colorimetry the human eye's sensitivity to light across the visible region is measured and a numerical description of colour is given. There are three attributes that are used to describe colour. The first identifies a colour by its location in the spectral sequence, *i.e*., what wavelength is associated with the colour. This is known as the hue, dominant wavelength, or chromatic colour, and is the wavelength where maximum contrast occurs. It is this aspect which is commonly, but mistakenly, referred to as colour. The second attribute, relating to the level of white and/or black, is known as saturation, chroma, tone, intensity, or purity. The third attribute is the brightness of the colour, also

referred to as value, lightness, or luminance. Luminance is very informative in considering the properties of electrochromes, because, with only one value, it provides information about the perceived transparency of a sample over the entire visible range. Since the introduction [7] of a simple *in situ* colorimetric analysis method for the precise control and measurement of colour in electrochromic systems, this approach has been successfully applied to the characterisation of 'type-III' [1] electrochromes, which remain as solid films under electrochromic operation. Thus, measurements have been made with numerous electrochromic conjugated polymer films and display devices prepared therefrom [8–13], and more recently to nickel oxide with various metal additives [14] and thin films of the intervalence charge-transfer complex Prussian blue (iron(III) hexacyanoferrate(II), PB) [15].

We here report the application of *in situ* colorimetric analysis to the study of the *N*,*N*´-bis(*n*-heptyl)-4,4´-bipyridylium ('di-*n*-heptyl viologen') system. The electrochromic properties of viologens have been intensively studied [1,16], and there is a long history of their use in prototype electrochromic display devices, since the first example reported in 1973 [17]. Viologen di-cations are colourless when pure unless optical charge transfer with the counter anion occurs. Reductive electron transfer forms the radical cation (see SCHEME 1 for di-*n*-heptyl viologen), the stability of which is attributable to the delocalisation of the radical electron throughout the π-framework of the bipyridyl nucleus.

SCHEME 1

Viologen radical cations are intensely coloured, with high molar absorption coefficients, owing to optical charge transfer between the (formally) +1 and zero valent nitrogens [1,16]. Suitable choice of nitrogen substituents in viologens to attain the appropriate molecular orbital energy levels allows colour choice of the radical cation, the di-*n*-heptyl viologen radical cation being purple. The intensity of the colour exhibited by di-reduced neutral

viologen species (SCHEME 1) is low since no optical charge transfer or internal transition corresponding to visible wavelengths is accessible.

Di-*n*-heptyl viologen was chosen for study here owing to its property as a 'type II' electrochrome [1,16], its soluble to insoluble transition on electrochemical reduction from aqueous solutions making it especially amenable to study by *in situ* colorimetry.

2. Experimental

2.1. Materials

Working electrode substrates were tin-doped indium oxide (ITO) on glass (7 x 50 x 0.7 mm, 5-15 Ω/□, part no. CG-50IN-CUV) from Delta Technologies Ltd.. Before each electrochemical investigation, ITO/glass substrates were pre-treated, in order to remove any trace of adhesive/impurities on the surface, by sonication (5 minutes) in a 1 mol dm^{-3} hydrochloric acid solution followed by rinsing with deionised water and air drying. *N*,*N*´-bis(*n*-heptyl)-4,4´-bipyridylium ('di-*n*-heptyl viologen') dibromide (as supplied, 97%) was recrystallised from water to yield pale yellow crystals. Potassium bromide (KBr) was a Fisher Scientific certified ACS reagent, and used without further purification.

2.2. Electrochemical measurements

Electrochemical measurements were carried out in de-oxygenated solutions (purged with pure argon) using an EG&G Model PAR 273A potentiostat/galvanostat, under the control of Scribner and Associates Corrware II software. No iR compensation was employed. For all measurements, a standard 1 cm quartz cuvette was used as the electrochemical cell. A machined polytetrafluoroethylene lid allowed the ITO/glass working electrode to be mounted transverse to the optical faces of the cuvette. Additional holes in the lid allowed a coiled platinum wire counter electrode and a reference electrode to be positioned in the electrolyte solution. A silver/silver bromide wire reference electrode was used, which, with aqueous 0.2 mol dm^{-3} KBr as supporting electrolyte, maintained a

stable potential of -0.086 V *vs*. a commercial BAS silver/silver chloride/saturated potassium chloride (+0.197 V *vs*. SHE) reference electrode. For all measurements, the lower 40 mm of each ITO/glass substrate was immersed in solution, providing a submerged geometric electrode active area of 2.80 cm^2. Adhesive copper tape at the top of each ITO/glass substrate provided the means for a uniform electrical contact.

2.3. In situ colorimetry

In situ colorimetric measurements, under potentiostatic control, were obtained using a Minolta CS-100 Chroma Meter and CIE (Commission Internationale de l'Eclairage) recommended normal/normal (0/0) illuminating/viewing geometry for transmittance measurements [18]. The calibration of the Chroma Meter was set to the preset mode. The standard illuminant was a D_{50} (5000 K) constant temperature daylight simulating light source in a light booth designed to exclude external light. Prior to each set of measurements, background colour coordinates (*Y*, *x*, and *y* values) were taken at open-circuit, using the blank ITO/glass substrate in the standard quartz cuvette containing the electrolyte solution under study. For measurements involving sequences of applied potentials, to ensure readings had equilibrated, colour coordinates were recorded after each potential had been applied for 50 seconds and the current had decayed to background levels. Additional readings were taken at 60 seconds, to ensure the colour coordinates had stabilised. For the experiments reported in section 3.3, readings were taken as a function of time under kinetic control. For all measurements, the ITO/glass substrate was on the side of the cuvette closest to the light source, with the conductive side facing the Chroma Meter. The *Yxy* values of the standard illuminant were converted to X_n, Y_n, Z_n tristimulus values [6], which, in turn, were used with the calculated tristimulus values (*X, Y, Z*) of each colour state for conversion to CIELAB *L*a*b** coordinates. The *x* and *y* coordinates were calculated from the *XYZ* tristimulus values using the formulae, $x = X/(X + Y + Z)$ and $y = Y/(X + Y + Z)$.

3. Results and discussion

3.1. Cyclic voltammetric and in situ colorimetric measurements with 0.5 x 10^{-3} mol dm^{-3} di-n-heptyl viologen in 0.2 mol dm^{-3} KBr solution

Initial measurements were undertaken to study the di-*n*-heptyl viologen system across both redox waves (SCHEME 1) using a relatively dilute solution. Fig. 1 shows cyclic voltammograms at 10, 100 and 500 mV s^{-1} across the region of electrochemical activity. In Fig. 1 (a), the peaks are labelled following the scheme of Bruinink et al. [19] who carried out an electrochemical investigation at tin oxide/glass electrodes of 0.2 cm^2 surface area. Bruinink et al. found that the number of peaks depends on experimental conditions such as scan speed and the age of the radical cation salt film. The peaks obtained here, albeit using ITO/glass electrodes of 2.80 cm^2 surface area, were consistent with the earlier studies. The main peaks a and a' are assigned to the formation of the purple radical cation salt on the ITO surface, followed by dissolution back to the di-cation. The main peak c is due to the second reduction step, which causes the formation of a yellow-brown deposit. Bruinink et al. [19], under their conditions, found the corresponding oxidation peak c' to only be present at > 100 mV s^{-1}, owing to the comproportionation chemical reaction (SCHEME 2), where the di-reduced neutral viologen species reacts with local viologen radical cation to generate further viologen radical cation.

SCHEME 2

In the present study, peak c' is present at each of the scan rates studied. Shoulder peaks b, connected with the second reduction step, and d and b', corresponding to oxidation of the viologen radical cation salt film, are consistent with the earlier study. In the present study, at low scan rate (Fig. 1 (a)) at -0.400 V, a shoulder, corresponding to reduction of adsorbed radical cation salt is also observed. This feature was observed in the electrochemical study of Belinko [20] on tin oxide/glass, but not in that of Bruinink et al. [19].

Table 1 shows *in situ* % colorimetric luminance (%*L*) and *xy* coordinates, as the potential is slowly stepped in sequence over the range 0.000 to –0.900 V, and then in reverse. Also shown at each applied potential are the calculated *L*a*b** coordinates, a uniform colour space (CIELAB) defined by the CIE in 1976. The CIE *L*a*b** space is a standard commonly used in the paint, plastic, and textile industries. *L** is the lightness variable of the sample, while *a** and *b** correspond to the two antagonistic chromatic processes (red-green and yellow-blue). In the *L*a*b** chromaticity diagram, + *a** is the red direction, – *a** is the green direction, + *b** is the yellow direction, and – *b** is the blue direction. The centre (0, 0) of the chromaticity diagram is achromatic; as the *a** and *b** values increase, the saturation of the colour increases. At the initial 0.000 V applied potential, the stable oxidation state is the colourless di-*n*-heptyl viologen di-cation, and the coordinates are coincident with those of the illumination source (the 'white point', where $x = 0.357$, $y = 0.383$, and $\%L = 100$). At –0.500, –0.600 and –0.700 V in the reduction direction, the ITO/glass surface is visually pale purple, due to the deposition of the di-*n*-heptyl viologen radical cation salt, in the region of potential expected from the cyclic voltammograms (Fig. 1). Measurement of the *L*a*b** coordinates allow this change to be followed, with a decrease in *L**, a positive change (towards red) in *a** and a negative change (towards blue) in *b**, quantifying the colour state (red + blue = purple). At –0.800 and –0.900 V, the ITO/glass surface appears yellow/brown due to the formation of the di-reduced di-*n*-heptyl viologen species. This potential range corresponds to that beyond peak c in the cyclic voltammograms (Fig. 1 (a)). Here, there is a small increase in the *L** variable, with a decrease in *a** and movement to a positive (towards yellow) value of *b**. On the reverse sequence, at –0.800 V the surface film switches from yellow-brown to pale purple, and then remains as pale pink at –0.700, –0.600, –0.500, –0.400 and –0.300 V. Calculation of the *L*a*b** coordinates allow quantification of each colour state (Table 1). The enhanced purple coloration on the reverse sequence (Table 1) is attributed to the

comproportionation reaction [21], where additional di-*n*-heptyl viologen radical cation salt is generated by reaction of the di-*n*-heptyl viologen di-cation and the di-reduced neutral di-*n*-heptyl viologen species (see SCHEME 2). Following 60 s at 0.000 V, the ITO/glass surface still remains purple, a further 240 s passing before the colour coordinates show full 'bleaching'. The persistence of the purple colour, following cycling to the di-reduced neutral viologen species is well known.

3.2. Cyclic voltammetric and in situ colorimetric measurements with 2 x 10^{-3} mol dm^{-3} di-n-heptyl viologen in 0.2 mol dm^{-3} KBr solution

Measurements were next taken using a higher concentration of di-*n*-heptyl viologen, in order to enhance changes in colour coordinates. Furthermore, the potential region was now restricted to the formation of the di-*n*-heptyl viologen radical cation, in order to avoid the complexities associated with the second reduction and the comproportionation reaction. Fig. 2 (a) shows the cyclic voltammogram of the system at 10 mV s^{-1}, a scan rate at which the features b' and f are resolved, in addition to the main peaks a and a'. Following colorimetric measurements (*vide infra*), minor changes in the cyclic voltammogram (Fig. 2 (b)) are found, due to the well-known aging of the surface film of di-*n*-heptyl viologen radical cation salt [19]. Peak f corresponds to oxidation of the aged, re-orientated, radical cation salt film, and was also seen, as a shoulder, in figs. 1 (b) and (c). At higher scan rates, where the radical cation salt film has less time to age, the cyclic voltammograms (Fig. 3) have a shape akin to that for a typical metal deposition/stripping electrochemical process. Analysis of potentiostatic current-time transients has been confirmed as a nice case of organic nucleation and subsequent crystal growth at SnO_2-coated electrode surfaces [22]. In the present work with ITO/glass substrates, rising current-time transients, diagnostic of nucleation and subsequent crystal growth, were likewise found for potentials between the Tafel and limiting current regions.

Table 2 shows *in situ* % colorimetric luminance (%*L*), *xy* and *L*a*b** coordinates, as the potential is slowly stepped in sequence over the range 0.000 to –0.600 V, and then in reverse. Preliminary measurements had established the appropriate intervals between applied potentials, as given in Table 2. Fig. 4 shows the *in situ* % colorimetric luminance (%*L*) data in graphical form. A sharp decrease in luminance is found on application of –0.425 V, a potential on the cyclic voltammogram (Fig. 3) between the Tafel and limiting current regions, on formation of the radical cation salt on the ITO/glass electrode surface. At –0.425 V, careful observation of the electrode by eye through the eye-piece of the colorimeter (with the benefit of illumination from the light source) reveals the colour of the electrodeposited film to start off as a uniform pale pink/purple. On maintaining the potential at –0.425 V, islands of deeper pink/purple are seen to form, which then slowly spread, until the film becomes fully uniform after 120 s. (For this specific potential, on the forward sequence, this additional time was allowed for stabilisation of the colour coordinates.) This observation represents visual confirmation of a mechanism that involves the growth of three-dimensional nuclei into a hemispherical diffusion zone [22]. Following the negative direction potential excursion, the % luminance was monitored in the positive potential direction (Fig. 4). Significant hysteresis was found, the stripping of the radical cation salt taking place ~0.1 to 0.2 V more positive of the original electrodeposition. This result is consistent with the voltammetric waveshape (Fig. 3).

Fig. 5 (a) shows the hue and saturation track in the *xy* chromaticity diagram for the di-*n*-heptyl viologen dication/radical cation transition, as the potential is slowly stepped between 0.000 and –0.600 V. In this figure and Fig. 5(b), only selected values from Table 2 are shown. The *xy* data (Table 2) for the –0.450 to –0.575 V forward sequence and the –0.575 to –0.400 V reverse sequence are excluded, due to the variable and small changes in this region. Although the *xy* chromaticity diagram is not a uniform colour space, abrupt changes in colour are found to correspond with significant changes in the *xy* coordinates.

The changes in *xy* coordinates in Fig. 5 occur as the colourless di-cationic viologen solution (at 0.000 V the *xy* coordinates are coincident with the 'white point') is reduced to yield the purple viologen radical cation salt on the ITO/glass. As noted for the luminance track, there is hysteresis in the *xy* coordinates. For the step-by-step reduction sequence, the main change there is a step change between –0.400 and –0.425 V. On the oxidation sequence the purple colour coordinates are maintained until beyond –0.400 V and then steady changes are observed in following each 0.025 V step to –0.300 V. In Fig. 5 (b), the *xy* data from Fig. 5 (a) are overlaid onto the CIE 1931 colour space template, showing the track of the *xy* coordinates between the white (transparent) and purple colour states. In this representation, the line surrounding the horse-shoe shaped area is called the spectral locus, giving the visible light wavelengths. The most saturated colours lie along the spectral locus. The line connecting the longest and shortest wavelength contains the non-spectral purples and is known as the purple line (Fig. 5 (b)). Surrounded by the spectral locus and the purple line is the region known as the colour locus, which contains every colour that can exist. The location of any point in the *xy* diagram gives the hue and saturation of the colour. For a given sample, the hue is determined by drawing a straight line through the point representing 'white' and the point of interest to the spectral locus, thus obtaining the dominant wavelength of the colour. For placing a wavelength dependence on a colour state such as that at –0.600 V (x = 0.378, y = 0.317) which is found along the purple line, a complementary wavelength (λ_c) can be expressed by drawing a straight line from the sample coordinate through the white point to the spectral locus. The construction shown in Fig. 5 (b) allows an estimated value of 548 nm, in excellent agreement with the wavelength (545 nm) of maximum absorbance in the visible region spectrum of the di-*n*-heptyl radical cation salt [23].

3.3. Dynamic in situ colorimetric measurements with 2 x 10^{-3} mol dm^{-3} di-n-heptyl viologen in 0.2 mol dm^{-3} KBr solution

To date, the study and interpretation of the *in situ* colorimetric analysis of electrochromic systems has only been carried out at applied potentials, following the attainment of equilibrium. The di-*n*-heptyl viologen system under study here, with the stated experimental conditions of solution concentrations, ITO/glass electrode area and cell geometry, had not been optimised in terms of maximising the switching speeds. Preliminary measurements established that the system switched colour sufficiently slowly to allow the demonstration of *in situ* colorimetry taking the manually obtained measurements in a dynamic fashion.

Following the study in *3.1* and *3.2* above, potentials of 0.000 and –0.425 V respectively, were chosen, corresponding to a value where the colourless di-*n*-heptyl viologen di-cation is the stable form and that where the electrodeposition of the radical cation salt can be steadily observed through changes in the colour coordinates. Fig. 6 (a) shows the steady track of the *xy* coordinates as the radical cation salt grows on the ITO/glass surface following a potential step from 0.000 to –0.425 V for 300 s. Fig. 6 (b) shows the steady decrease in relative luminance over the 300 s corresponding to the increase of light absorbed. Following switching to open-circuit at 300 s, the colour coordinates revert to those of the colourless radical cation after a further 100 s (Fig. 6 (b) for the luminance data). Although, as noted, all solutions were purged with argon prior to measurements, the bleaching observed at open-circuit is interpreted as the regeneration of the di-*n*-heptyl viologen di-cation form by chemical reaction of the radical cation salt with extraneous trace ambient oxygen. Fig. 6 (c) shows the relative luminance data following a square-wave potential step from 0.000 to –0.425 V (300 s) and then to 0.000 V (100 s). The rapid bleaching observed visually, and through the measurements of the colour coordinates,

is consistent with the relatively sharp ‘stripping’ peak observed in the cyclic voltammograms.

Conclusion

An *in situ* colorimetric method, based on the CIE (Commission Internationale de l'Eclairage) system of colorimetry, has been successfully applied to the study of the electrochromic *N*,*N*´-bis(*n*-heptyl)-4,4´-bipyridylium (‘di-*n*-heptyl viologen’) system. The technique is a convenient method for the precise measurement of the hue, saturation and luminance of colour states and allows the changes in these properties to be carefully monitored on redox switching between electrochromic colour states. Significant hysteresis was found for the di-*n*-heptyl viologen system. For this ‘type II’ electrochrome system, the precise colour exhibited at a specific potential depends on the polarity direction of the sequence of applied potentials. The di-*n*-heptyl viologen di-cation/radical cation salt electrodeposition/stripping process was sufficiently slow, to allow, for the first time, the demonstration of *in situ* colorimetry measurements in a kinetic mode.

Acknowledgements

We thank the EPSRC for an Overseas Travel Grant (EP/E000746/1) to RJM and the AFOSR (FA9550-06-1-0192) for financial support.

References

[1] P.M.S. Monk, R.J. Mortimer, D.R. Rosseinsky, Electrochromism and Electrochromic Devices, Cambridge University Press, Cambridge, 2007.

[2] C.G. Granqvist, Handbook of Inorganic Electrochromic Materials, Elsevier, Amsterdam, 1995.

[3] R.J. Mortimer, A.L. Dyer, J.R. Reynolds, Electrochromic organic and polymeric materials for display applications, Displays, 27 (2006) 2–18.

[4] R.M. Christie, Colour Chemistry, Royal Society of Chemistry, Cambridge, 2001, ch. 2.

[5] R.G. Kuehni, Color: An Introduction to Practice and Principles, 2nd edn., J. Wiley & Sons, Inc., Hoboken, New Jersey, 2005.

[6] G. Wyszecki, W.S. Stiles, Color Science: Concepts and Methods, Quantitative Data and Formulae, J. Wiley & Sons, New York, 2nd edn., 1982.

[7] B.C. Thompson, P. Schottland, K. Zong, J. R. Reynolds, In situ colorimetric analysis of electrochromic polymers and devices, Chem. Mater. 12 (2000) 1563–1571.

[8] B.C. Thompson, P. Schottland, G. Sönmez, J. R. Reynolds, In situ colorimetric analysis of electrochromic polymer films and devices, Synth. Met. 119 (2001) 333–334.

[9] I. Schwendeman, R. Hickman, G. Sönmez, P. Schottland, K. Zong, D. M. Welsh, J. R. Reynolds, Enhanced contrast dual polymer electrochromic devices, Chem. Mater. 14 (2002) 3118–3122.

[10] G. Sönmez, I. Schwendeman, P. Schottland, K. Zong, J.R. Reynolds, N-Substituted poly(3,4-propylenedioxypyrrole)s: High gap and low redox potential switching electroactive and electrochromic polymers, Macromolecules 36 (2003) 639–647.

[11] A. Cirpan, A.A. Argun, C.R.G. Grenier, B.D. Reeves, J.R. Reynolds, J. Mater. Chem., Electrochromic devices based on soluble and processable dioxythiophene polymers, 13 (2003) 2422–2428.

[12] G. Sönmez, H. Meng, F Wudl, Chem. Mater., Organic polymeric electrochromic devices: polychromism with very high coloration efficiency, 16 (2004) 574–.

[13] C.A. Thomas, K. Zong, K.A. Abboud, P.J. Steel, J.R. Reynolds, Donor-mediated band gap reduction in a homologous series of conjugated polymers, J. Am. Chem. Soc. 126 (2004) 16440–16450.

[14] E. Avendaño, A. Azens, G.A. Niklasson, C.G. Granqvist, Electrochromism in nickel oxide films containing Mg, Al, Si, V, Zr, Nb, Ag, or Ta, Sol. Energy Mater. Sol. Cells 84 (2004) 337–350.

[15] R.J. Mortimer, J.R. Reynolds, In situ colorimetric and composite coloration efficiency measurements for electrochromic Prussian blue, J. Mater. Chem. 15 (2005) 2226–2233.

[16] P.M.S. Monk, The Viologens: Physicochemical Properties, Synthesis and Applications of the Salts of 4,4´-Bipyridine, J. Wiley & Sons, Chichester, 1998.

[17] C.J. Schoot, J.J. Ponjee, H.T. van Dam, R.A. van Doorn, P.J. Bolwijn, New electrochromic display, Appl. Phys. Lett. 23 (1973) 64–65.

[18] R.T. Marcus, in Color for Science, Art, and Technology, ed. K. Nassau, Elsevier, Amsterdam, 1998, pp. 31–96.

[19] J. Bruinink, C.G.A. Kregting, J.J. Ponjeé, Modified viologens with improved electrochemical properties for display applications, J. Electrochem. Soc. 124 (1977) 1854–1858.

[20] K. Belinko, Electrochemical studies of the viologen system for display applications, Appl. Phys. Lett. 29 (1976) 363–365.

[21] D.R. Rosseinsky, P.M.S. Monk, Comproportionation in propylene carbonate of substituted bipyridyliums. Rates and equilibria by rotating ring-disc electrode and associated electrochemical studies, J. Chem. Soc., Faraday Trans. 89 (1993) 219–222.

[22] S. Fletcher, L. Duff, R.G. Barradas, Nucleation and charge-transfer kinetics at the viologen/SnO_2 interface in electrochromic device applications, J. Electroanal. Chem. 100 (1979) 759–770.

[23] N.J. Goddard, A.C. Jackson, M.G. Thomas, Spectroelectrochemical studies of some viologens used in electrochromic display applications, J. Electroanal. Chem. 159 (1983) 325–335.

Figure legends

Fig. 1

Cyclic voltammograms at 10 (Fig. 1 (a)), 100 (Fig. 1 (b)) and 500 (Fig. 1 (c)) mV s^{-1} scan rate for an ITO/glass electrode in aqueous 0.5 x 10^{-3} mol dm^{-3} di-*n*-heptyl viologen dibromide/0.2 mol dm^{-3} KBr. Initial potential, 0.000 V *vs.* Ag/AgBr. Return potential – 0.900 V vs. Ag/AgBr. Arrows indicate direction of potential scan.

Fig. 2

Cyclic voltammogram at 10 mV s^{-1} scan rate for an ITO/glass electrode in aqueous 2 x 10^{-3} mol dm^{-3} di-*n*-heptyl viologen dibromide/0.2 mol dm^{-3} KBr. Initial potential, 0.000 V *vs.* Ag/AgBr. Return potential –0.600 V vs. Ag/AgBr. Arrows indicate direction of potential scan. Fig. 2 (a) is for a fresh ITO/glass electrode and Fig. 2 (b) is for the same ITO/glass electrode, following a set of *in situ* colorimetry measurements.

Fig. 3

Cyclic voltammogram at 50, 100 and 200 mV s^{-1} scan rate for an ITO/glass electrode in aqueous 2 x 10^{-3} mol dm^{-3} di-*n*-heptyl viologen dibromide/0.2 mol dm^{-3} KBr. Initial potential, 0.000 V *vs.* Ag/AgBr. Return potential –0.600 V vs. Ag/AgBr. Arrows indicate direction of potential scan.

Fig. 4

Relative luminance (%), *vs.* applied potential (*E*/V *vs*. Ag/AgBr) for reduction/oxidation of the di-*n*-heptyl viologen system from 2 x 10^{-3} mol dm^{-3} di-*n*-heptyl viologen dibromide/0.2 mol dm^{-3} KBr at an ITO/glass substrate. The initial potential was 0.000 V and the potential was stepped to the values indicated in Table 2. The arrows indicate the direction of the changes with potential.

Fig. 5

CIE 1931 *xy* chromaticity diagrams for reduction/oxidation of the di-*n*-heptyl viologen system from 2 x 10^{-3} mol dm^{-3} di-*n*-heptyl viologen dibromide/0.2 mol dm^{-3} KBr at an

ITO/glass substrate. The initial potential was 0.000 V and the potential was stepped to the values indicated in Table 2. The arrows indicate the direction of the changes with potential. In Fig. 5 (b), the *xy* coordinates are plotted onto a diagram that shows the locus coordinates, with labelled hue wavelengths, and the evaluation of the complementary wavelength (λ_c) of the film of di-*n*-heptyl viologen radical cation salt at –0.600 V.

Fig. 6

CIE 1931 *xy* coordinates (Fig. 6 (a)) and relative luminance (%) data as a function of time, following the application of a potential step from 0.000 to -0.425 V vs. Ag/AgBr in 2 x 10^{-3} mol dm^{-3} di-*n*-heptyl viologen dibromide/0.2 mol dm^{-3} KBr at an ITO/glass substrate. Additional relative luminance (%) data are plotted following the switch at 300 s to open-circuit (Fig. 6 (b)) and 0.000 V (Fig. 6 (c)) respectively.

Table 1

Colorimetry coordinates for reduction/oxidation of the di-*n*-heptyl viologen system from 0.5 x 10^{-3} mol dm^{-3} di-*n*-heptyl viologen dibromide/0.2 mol dm^{-3} KBr at an ITO/glass substrate

E/V vs. Ag/AgBr	%*L*	*x*	*y*	*L**	*a**	*b**
0.000	100.0	0.357	0.383	100	0	0
–0.300	99.1	0.358	0.384	100	0	1
–0.400	97.2	0.358	0.384	99	0	1
–0.500	77.7	0.356	0.362	91	8	-9
–0.600	79.7	0.357	0.362	92	9	-8
–0.700	70.4	0.357	0.357	87	11	-10
–0.800	85.0	0.368	0.39	94	2	6
–0.900	83.6	0.368	0.384	93	4	3
–0.800	77.0	0.368	0.378	90	7	1
–0.700	63.0	0.365	0.357	83	13	-8
–0.600	56.4	0.362	0.338	80	20	-15
–0.500	56.8	0.361	0.338	80	19	-16
–0.400	62.2	0.36	0.344	83	17	-14
–0.300	70.2	0.358	0.356	87	11	-10
0.000	95.3	0.358	0.383	98	0	0

Table 2

Colorimetry coordinates for reduction/oxidation of the di-*n*-heptyl viologen system from 2 x 10^{-3} mol dm^{-3} di-*n*-heptyl viologen dibromide/0.2 mol dm^{-3} KBr at an ITO/glass substrate. The *xy* coordinates in bold are plotted in figure 5.

E/V vs. Ag/AgBr	%*L*	*x*	*y*	*L**	*a**	*b**
0.000	**96.3**	**0.360**	**0.386**	**99**	**–1**	**2**
–0.350	**96.3**	**0.360**	**0.386**	**99**	**–1**	**2**
–0.375	**95.6**	**0.360**	**0.386**	**98**	**–1**	**2**
–0.400	**93.3**	**0.361**	**0.384**	**97**	**0**	**1**
–0.425	**49.9**	**0.378**	**0.316**	**76**	**34**	**–20**
–0.450	50.6	0.377	0.317	76	33	–20
–0.475	50.7	0.378	0.317	77	33	–20
–0.500	54.9	0.375	0.324	79	30	–19
–0.525	53.3	0.376	0.321	78	31	–19
–0.550	52.3	0.376	0.319	77	32	–20
–0.575	51.4	0.377	0.318	77	33	–20
–0.600	**50.8**	**0.378**	**0.317**	**77**	**33**	**–20**
–0.575	50.4	0.378	0.316	76	34	–20
–0.550	50.3	0.378	0.316	76	34	–20
–0.525	50.1	0.378	0.316	76	34	–20
–0.500	50.0	0.379	0.316	76	34	–20
–0.475	49.8	0.379	0.316	76	34	–20
–0.450	49.7	0.379	0.316	76	34	–20
–0.425	49.7	0.379	0.316	76	34	–20
–0.400	49.7	0.378	0.316	76	34	–20
–0.375	**50.2**	**0.377**	**0.318**	**76**	**32**	**–20**
–0.350	**56.4**	**0.371**	**0.332**	**80**	**25**	**–16**
–0.325	**77.8**	**0.362**	**0.369**	**91**	**7**	**–5**
–0.300	**88.9**	**0.360**	**0.383**	**96**	**0**	**0**
0.000	**92.6**	**0.360**	**0.386**	**97**	**–1**	**2**

Fig. 1 (a), (b) and (c)

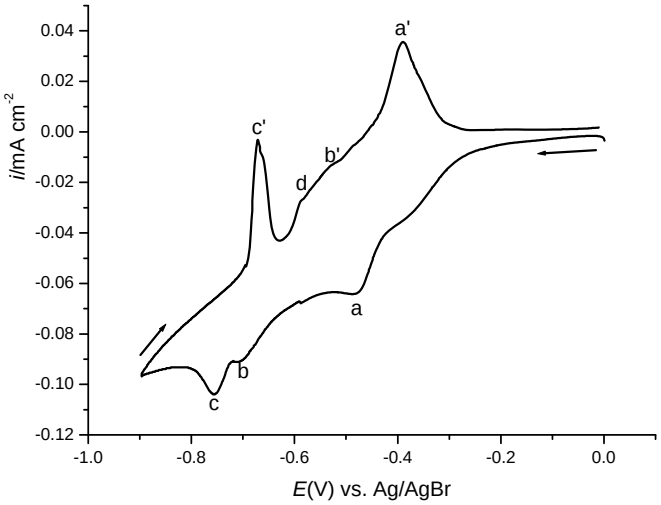
a'
c'
b'
d
a
b
c
0.04
0.02
0.00
-0.02
-0.04
-0.06
-0.08
-0.10
-0.12
-1.0
-0.8
-0.6
-0.4
-0.2
0.0
i/mA cm-2
E(V) vs. Ag/AgBr

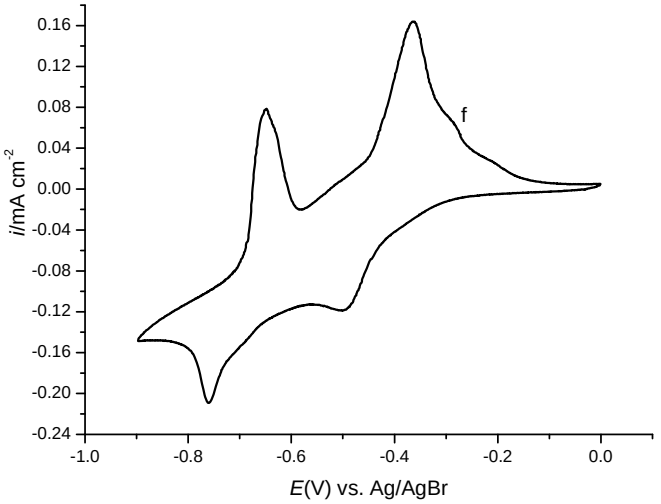
f
0.16
0.12
0.08
0.04
0.00
-0.04
-0.08
-0.12
-0.16
-0.20
-0.24
-1.0
-0.8
-0.6
-0.4
-0.2
0.0
i/mA cm-2
E(V) vs. Ag/AgBr

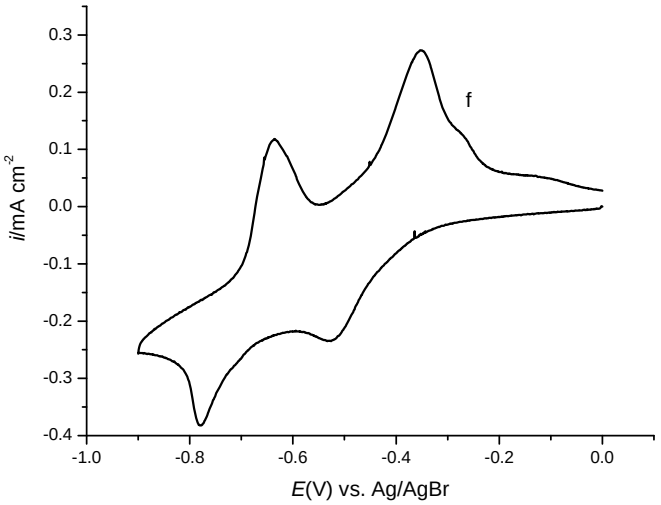
f
0.3
0.2
0.1
0.0
-0.1
-0.2
-0.3
-0.4
-1.0
-0.8
-0.6
-0.4
-0.2
0.0
i/mA cm-2
E(V) vs. Ag/AgBr

Fig. 2

(a)

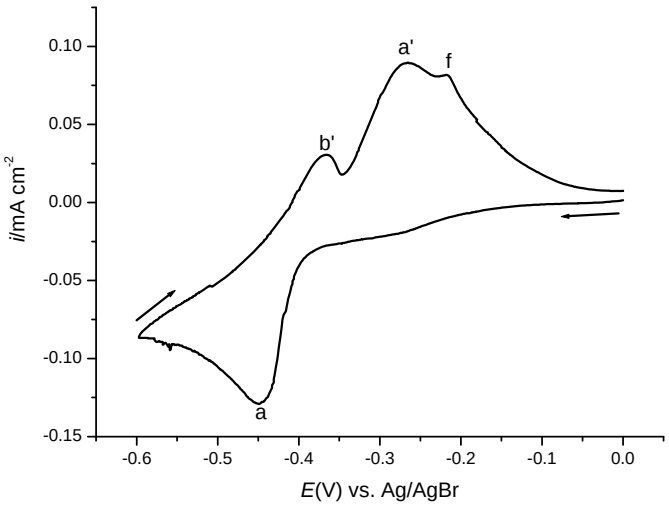
0.10
0.05
0.00
-0.05
-0.10
-0.15
-0.6
-0.5
-0.4
-0.3
-0.2
-0.1
0.0
a'
f
b'
a
i/mA cm-2
E(V) vs. Ag/AgBr

(b)

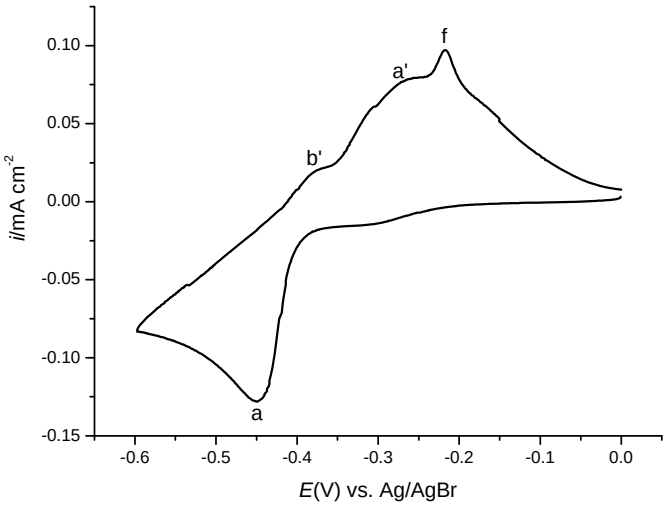
0.10
0.05
0.00
-0.05
-0.10
-0.15
-0.6
-0.5
-0.4
-0.3
-0.2
-0.1
0.0
f
a'
b'
a
i/mA cm-2
E(V) vs. Ag/AgBr

Fig. 3

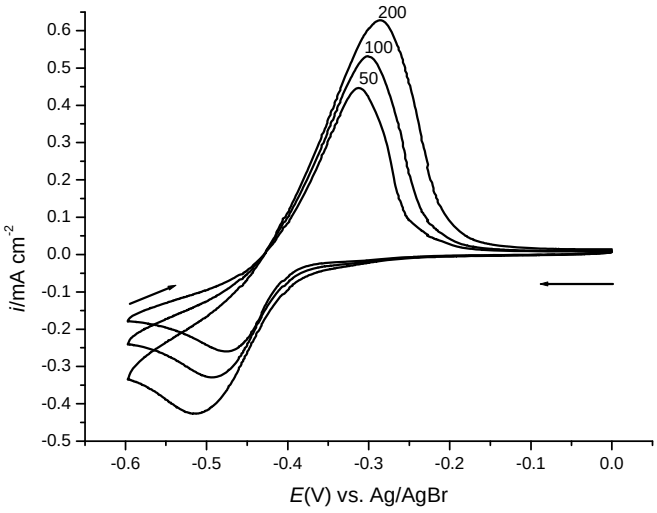
200
100
50
0.6
0.5
0.4
0.3
0.2
0.1
0.0
-0.1
-0.2
-0.3
-0.4
-0.5
-0.6
-0.5
-0.4
-0.3
-0.2
-0.1
0.0
i/mA cm-2
E(V) vs. Ag/AgBr

Fig. 4

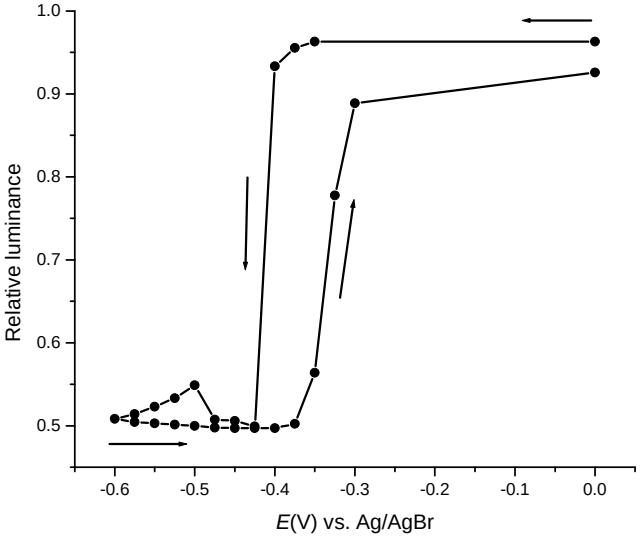
1.0
0.9
0.8
0.7
0.6
0.5
-0.6
-0.5
-0.4
-0.3
-0.2
-0.1
0.0
Relative luminance
E(V) vs. Ag/AgBr

Fig. 5

(a)

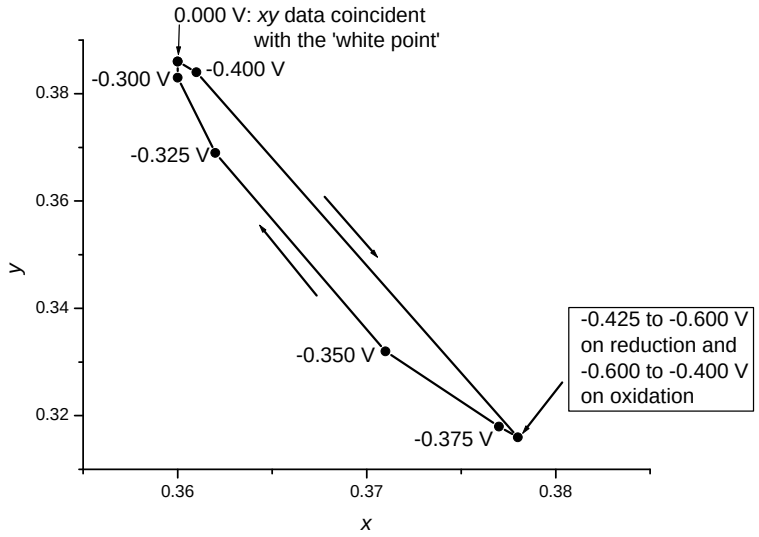
0.000 V: xy data coincident
with the 'white point'
-0.300 V
-0.400 V
-0.325 V
-0.350 V
-0.375 V
-0.425 to -0.600 V
on reduction and
-0.600 to -0.400 V
on oxidation
0.38
0.36
0.34
0.32
y
0.36
0.37
0.38
x

(b)

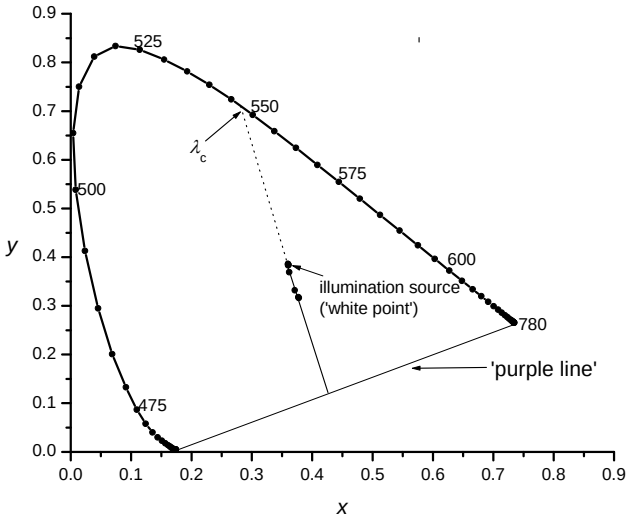
525
550
λc
575
500
600
illumination source
('white point')
780
'purple line'
475
y
x

Fig. 6 (a), (b) and (c)

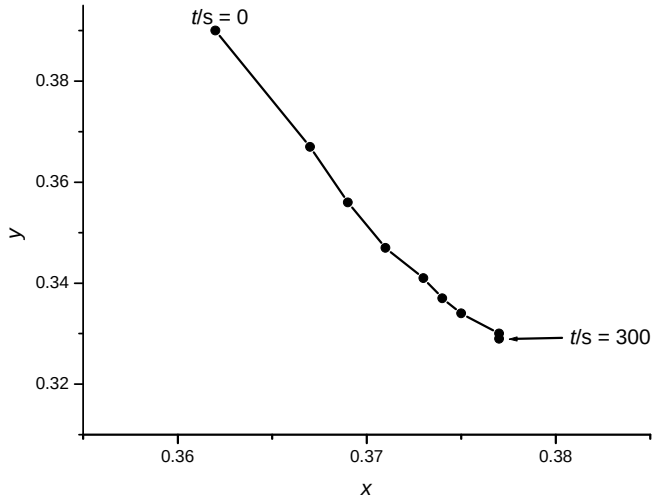
t/s = 0
t/s = 300
0.38
0.36
0.34
0.32
y
0.36
0.37
0.38
x

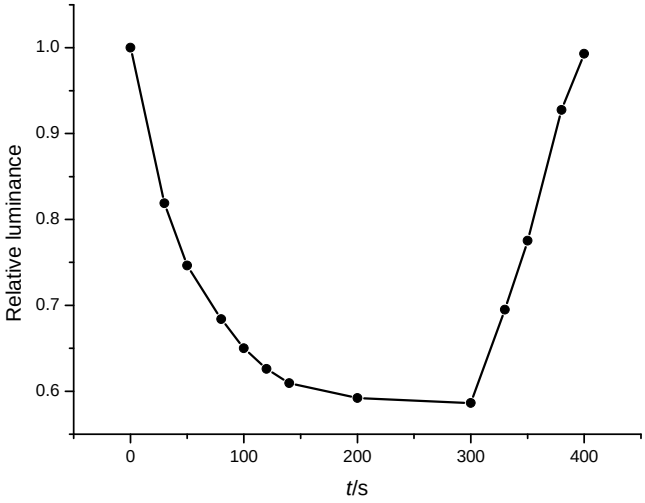
1.0
0.9
0.8
0.7
0.6
Relative luminance
0
100
200
300
400
t/s

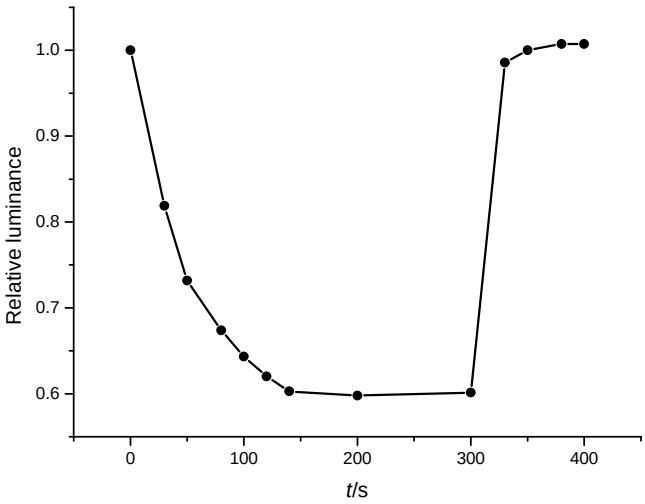
1.0
0.9
0.8
0.7
0.6
Relative luminance
0
100
200
300
400
t/s

SCHEME 1

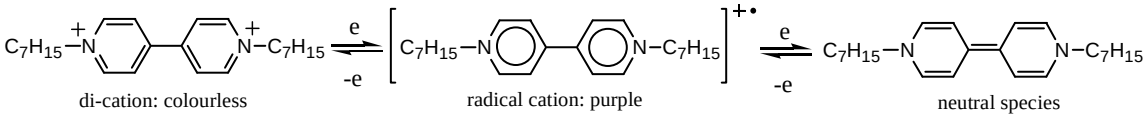

SCHEME 2